ЖЭТФ, 2009, том 136, вып. 4 (10), стр. 797–810

OPTICAL EDGE MODES IN PHOTONIC LIQUID CRYSTALS

V. A. Belyakov [a]*, ***S. V. Semenov*** [b]

[a] *Landau Institute for Theoretical Physics, Russian Academy of Sciences*
142432, Chernogolovka, Moscow Region, Russia

[b] *Russian Research Center "Kurchatov Institute"*
123182, Moscow, Russia

Received March 30, 2009

An analytic theory of localized edge modes in chiral liquid crystals (CLCs) is developed. Equations determining the edge-mode frequencies are found and analytically solved in the case of low decaying modes and are solved numerically for the problem parameter values typical for the experiment. The discrete edge-mode frequencies specified by the integer numbers n are located close to the stop-band edge frequencies outside the band. The expressions for the spatial distribution of the n's mode field in a CLC layer and for its temporal decay are presented. The possibilities of a reduction of the lasing threshold due to the anomalously strong absorption effect are theoretically investigated for a distributed feedback lasing in CLCs. It is shown that a minimum of the threshold pumping wave intensity may be reached, generally, for the pumping wave propagating at an angle to the helical axis. However, for lucky values of the related parameters, it may be reached for the pumping wave propagating along the helical axis. The lowest threshold pumping wave intensity occurs for the lasing at the first low-frequency band-edge lasing mode and the pumping wave propagating at an angle to the spiral axis corresponding to the first angular absorption maximum of the anomalously strong absorption effect at the high-frequency edge of the stop band. The study is performed in the case of the average dielectric constant of the liquid crystal coinciding with the dielectric constant of the ambient material. Numerical calculations of the distributed feedback lasing threshold at the edge-mode frequencies are performed for typical values of the relevant parameters.

PACS: 42.70.Qs, 42.70.Df

1. INTRODUCTION

Recently, there was an explosion of interest in the mirrorless distributed feedback (DFB) lasing in chiral liquid crystals (CLCs) [1]. The reason for this interest is related to the observed low-threshold lasing [2, 3], unusual polarization properties of lasing, and frequency tunability of the lasing by means of applying an external field [4, 5], temperature pitch variations [6, 7], or mechanical stress [8], etc.

The DFB low-threshold lasing in CLCs occurs at frequencies close to the frequencies of the stop-band edges [2–8]. The corresponding frequencies were associated with so-called edge lasing modes [1]. It also happens that at the same edge lasing mode frequencies, an anomalously strong absorption of the pumping wave occurs [9–13].

In general, the theory of edge lasing modes in CLCs (and the more general DFB lasing in spiral media) is very similar to the corresponding theory for conventional periodic solid media that was initially developed by Kogelnik and Shank [14] in the coupled-wave approximation and was later treated similarly in many papers (see [15] and the references therein). But the theory of edge lasing modes in CLCs deserves a separate study because of unusual optical properties of CLCs and because, in contrast to all other periodic media, an exact analytic solution of the Maxwell equations is known for CLCs (and more generally, for spiral media). Many related results, usually obtained in a numerical approach, may therefore be obtained analytically for CLCs. For example, the anomalously strong absorption effect existing in CLCs [9, 10] for the light frequency close to the stop band may be treated analytically. (The anomalously strong absorption effect

*E-mail: bel@landau.ac.ru

for conventional periodic media was also studied in Ref. [16].)

General analytic expressions for the solution of the boundary problem for the nonabsorbing, absorbing, and amplifying CLC layers, i. e., for the edge modes (EMs), are presented below for the light propagation direction coinciding with the spiral axis. We find the dispersion equation for EMs determining their frequencies; the lasing threshold gain is found and an expression for the threshold in a specific limit case is also presented together with numerical solutions of the dispersion equation for typical values of the CLC parameters. The EM properties (coordinate intensity distribution, frequency width of the EM, etc.) are analyzed. It is also discussed how the revealed properties of EMs allow decreasing the DFB lasing threshold ensured by a low gain for the lasing and a strong absorption for the pumping wave.

2. EIGENWAVES IN CLC

To solve the boundary value problem related to EMs, we need to know eigenwaves in a CLC. As is known [10, 17–19], the eigenwaves corresponding to propagation of light in a CLC along a spiral axis z, i. e., the solutions of the Maxwell equation

$$\frac{\partial^2 \mathbf{E}}{\partial z^2} = \frac{\varepsilon(z)}{c^2}\frac{\partial^2 \mathbf{E}}{\partial t^2}, \tag{1}$$

are given by a superposition of two plane waves of the form

$$\mathbf{E}(z,t) = e^{-i\omega t} \times \\ \times \left[E^+ \mathbf{n}_+ \exp(iK^+ z) + E^- \mathbf{n}_- \exp(iK^- z)\right]. \tag{2}$$

Here, ω is the light frequency, c is the speed of light, $\mathbf{n}_\pm = (\mathbf{e}_x \pm \mathbf{e}_y)/\sqrt{2}$ are circular polarization vectors with $\mathbf{e}_x$ and $\mathbf{e}_y$ being the unit vectors along the x and y axes, and

$$\varepsilon(z) = \\ = \begin{pmatrix} \varepsilon_0\left[1+\delta\cos(\tau z)\right] & \pm\varepsilon_0\delta\sin(\tau z) & 0 \\ \pm\varepsilon_0\delta\sin(\tau z) & \varepsilon_0\left[1-\delta\cos(\tau z)\right] & 0 \\ 0 & 0 & \varepsilon_\perp \end{pmatrix} \tag{3}$$

is the dielectric tensor of the CLC [10, 17–19] (two signs in the expression for $\varepsilon(z)$ correspond to the right and left chirality of the CLC), where $\varepsilon_0 = (\varepsilon_\parallel + \varepsilon_\perp)/2$, $\delta = (\varepsilon_\parallel - \varepsilon_\perp)/(\varepsilon_\parallel + \varepsilon_\perp)$ is the dielectric anisotropy, and

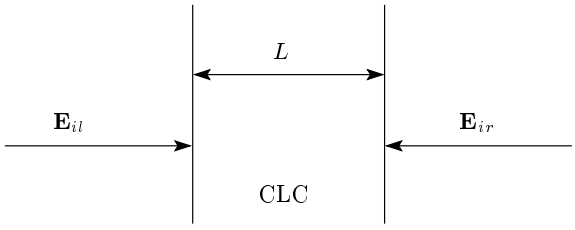

Fig. 1. Schematic of the boundary value problem for edge modes

$\varepsilon_\parallel$ and $\varepsilon_\perp$ are the local principal values of the CLC dielectric tensor [9, 16, 17]. The wave vectors $K^\pm$ satisfy the condition

$$K^+ - K^- = \tau, \tag{4}$$

where τ is the reciprocal lattice vector of the LC spiral ($\tau = 4\pi/p$, where p is the cholesteric pitch).

The wave vectors $K^\pm$ in four eigensolutions of Eq. (1) are determined by Eq. (3) and the formulas

$$K_j^+ = \frac{\tau}{2} \pm \kappa\sqrt{1 + \left(\frac{\tau}{2\kappa}\right)^2 \pm \sqrt{\left(\frac{\tau}{\kappa}\right)^2 + \delta^2}}, \tag{5}$$

where j labels the eigensolutions with the ratio of the amplitudes E^-/E^+ given by

$$\left(\frac{E^-}{E^+}\right)_j = \delta\left[(K_j^+ - \tau)^2/\kappa^2 - 1\right]^{-1}, \tag{6}$$

where $\kappa = \omega\sqrt{\varepsilon_0}/c$. We do not specify the kind of the CLC under investigation here (chiral smectic or cholesteric) because the optics of light propagating along the spiral axis is identical for both LC types [10, 17–20]. For definiteness, we give the expressions for cholesterics below. The corresponding expressions for chiral smectics can be obtained by a simple redefinition of the relevant parameters (see Ref. [10, Ch. 2]).

Two of the eigenwaves corresponding to the circular polarization with the sense of chirality coinciding with the one of the CLC spiral experience strong diffraction scattering at the frequencies in the region of the stop band. The other two eigenwaves corresponding to the opposite circular polarizations are almost unaffected the diffraction scattering even at the frequencies of the stop band for the former circular polarization.

Because, as we see in what follows, the specific features of EMs in the CLC are related to eigenwaves of the diffracting polarization, we limit ourselves by considering the propagation of light of the diffracting polarization only in the CLC.

3. BOUNDARY VALUE PROBLEM

To investigate EMs in a CLC, we have to consider a boundary value problem. We assume that the CLC is represented by a planar layer with the spiral axis perpendicular to the layer surfaces (Fig. 1). To justify our intention to limit ourselves by propagation of light of the diffracting polarization only, we also assume that the average CLC dielectric constant ε_0 coincides with the dielectric constant of the ambient medium. This assumption practically prevents conversion of one circular polarization into another at layer surfaces [10, 21] and allows taking only two eigenwaves with diffracting circular polarization into account.

We begin with the linear boundary value problem in the formulation where two plane waves of the diffracting polarization and of the same frequency are incident along the spiral axis at the layer from the opposite sides (see Fig. 1) and the dielectric tensor can have a nonzero imaginary part of any sign (which means that the CLC layer may be either absorbing or amplifying). The amplitudes E_j^+ of the two diffracting eigenwaves excited in the layer by the incident waves (they are denoted by E_+^+ and E_-^+) are determined by the equations

$$\begin{gathered} E_+^+ + E_-^+ = E_{ir}, \\ \exp(iK_+^+L)\delta\left[(K_+^+ - \tau)^2/\kappa^2 - 1\right]^{-1} E_+^+ + \\ + \exp(iK_-^+L)\delta\left[(K_-^+ - \tau)^2/\kappa^2 - 1\right]^{-1} E_-^+ = E_{il}, \end{gathered} \tag{7}$$

where E_{ir} and E_{il} are the amplitudes of the waves incident at the layer from the right and from the left, L is the layer thickness, and

$$K_\pm^+ = \frac{\tau}{2} \pm \kappa\sqrt{1 + \left(\frac{\tau}{2\kappa}\right)^2 - \sqrt{\left(\frac{\tau}{\kappa}\right)^2 + \delta^2}}\,. \tag{8}$$

The amplitudes of waves exiting from the layer on the right and the left sides, E_{er} and E_{el}, are determined by the expressions

$$\begin{gathered} E_{er} = \delta\left[(K_+^+ - \tau)^2/\kappa^2 - 1\right]^{-1} E_+^+ + \\ + \delta\left[(K_-^+ - \tau)^2/\kappa^2 - 1\right]^{-1} E_-^+, \\ E_{el} = \exp\left[i(K_+^+ - \kappa)L\right] E_+^+ + \\ + \exp\left[i(K_-^+ - \kappa)L\right] E_-^+. \end{gathered} \tag{9}$$

If we assume that the amplitude of only one incident wave is nonzero, Eqs. (9) determines the reflected and transmitted waves (the reflection R and transmission T coefficients of the layer) and, in particular, their frequency dependence [10, 19, 21]. The corresponding expressions for R and T take the form

$$\begin{gathered} R = \\ = \frac{\delta^2 |\sin(qL)|^2}{\left|\dfrac{q\tau}{\kappa^2}\cos(qL) + i\left[\left(\dfrac{\tau}{2\kappa}\right)^2 + \left(\dfrac{q}{\kappa}\right)^2 - 1\right]\sin(qL)\right|^2}, \\ T = \\ = \frac{|\exp(i\kappa L)(q\tau/\kappa^2)|^2}{\left|\dfrac{q\tau}{\kappa^2}\cos(qL) + i\left[\left(\dfrac{\tau}{2\kappa}\right)^2 + \left(\dfrac{q}{\kappa}\right)^2 - 1\right]\sin(qL)\right|^2}, \end{gathered} \tag{10}$$

where

$$q = \kappa\sqrt{1 + \left(\frac{\tau}{2\kappa}\right)^2 - \sqrt{\left(\frac{\tau}{\kappa}\right)^2 + \delta^2}}\,. \tag{11}$$

If both amplitudes of the incident waves are equal to zero, no waves emerging from the layer exist if the dielectric tensor has a positive (or a very small negative) imaginary part.

The solution of system (7) for the amplitudes E_+^+ and E_-^+ of the eigenwaves in the CLC layer is given by the following expressions (in the case of a wave incident only on one surface of the layer):

$$\begin{gathered} E_+^+ = -E_{il}\exp(-iqL)\times \\ \times\frac{(\tau/2\kappa)^2 + (q/\kappa)^2 - 1 - q\tau/\kappa^2}{2\left\{\dfrac{q\tau}{\kappa^2}\cos(qL) + i\left[\left(\dfrac{\tau}{2\kappa}\right)^2 + \left(\dfrac{q}{\kappa}\right)^2 - 1\right]\sin(qL)\right\}}, \\ E_-^+ = E_{il}\exp(iqL)\times \\ \times\frac{(\tau/2\kappa)^2 + (q/\kappa)^2 - 1 + q\tau/\kappa^2}{2\left\{\dfrac{q\tau}{\kappa^2}\cos(qL) + i\left[\left(\dfrac{\tau}{2\kappa}\right)^2 + \left(\dfrac{q}{\kappa}\right)^2 - 1\right]\sin(qL)\right\}}. \end{gathered} \tag{12}$$

The values of the eigenwave amplitudes close to the stop-band edges are strongly oscillating functions of frequency (see Figs. 2 and 3 presenting the calculation results). At the points of maxima close to the stop-band edges, their values are much larger than the incident wave amplitude E_{il}. It turns out that the amplitude maxima frequencies coincide with the frequencies of zero reflection following from Eqs. (10) for a nonabsorbing CLC (Figs. 2 and 3).

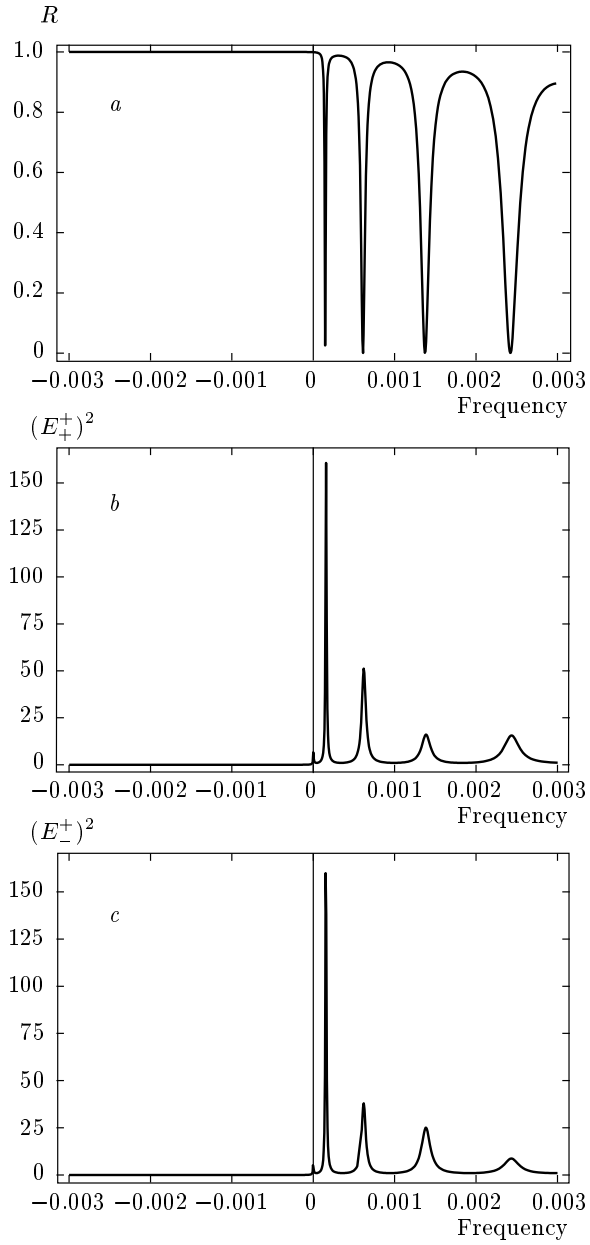

Fig. 2. Reflection coefficient R (a) and the squared E_+^+ (b) and E_-^+ (c) eigenmode amplitudes calculated versus frequency for a nonabsorbing CLC layer ($\delta = 0.05$, $N = L/p = 250$). Here and in all figures below (except Fig. 11), $\delta(\nu - 1)$ is plotted at the frequency axis, i. e., the frequency deviation from the stop-band edge is plotted (normalized by the Bragg frequency, see Eq. (23))

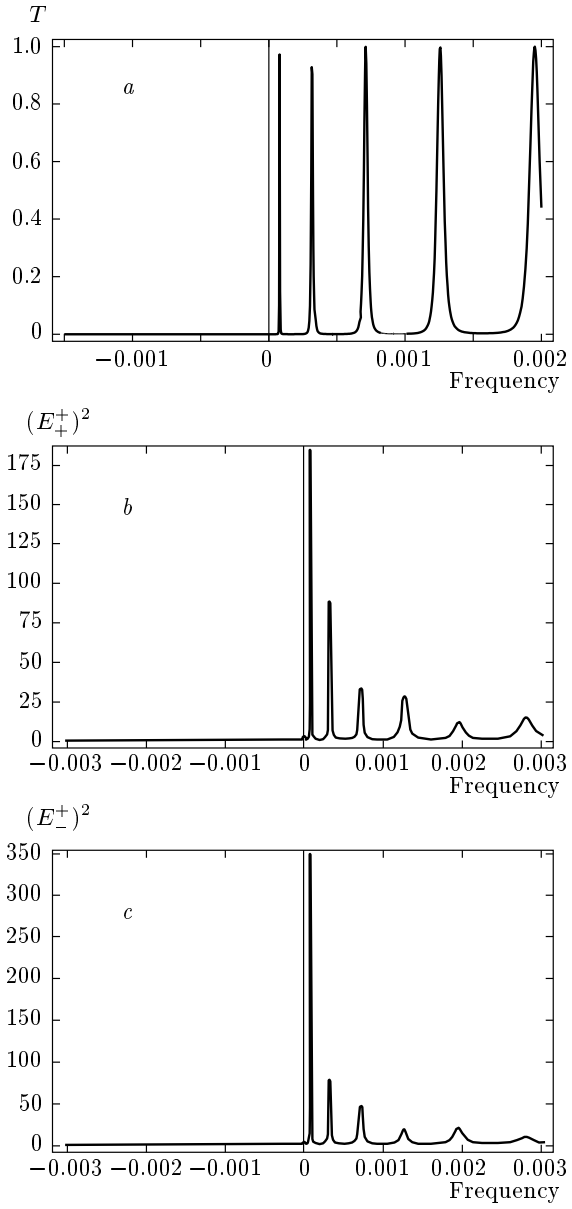

Fig. 3. Transmission coefficient T (a) and the squared E_+^+ (b) and E_-^+ (c) eigenmode amplitudes calculated versus frequency for a nonabsorbing CLC layer ($\delta = 0.05$, $N = 350$)

4. EDGE MODES (NONABSORBING CLC)

We examine the formulas of the preceding section for a nonabsorbing CLC in more detail. In a nonabsorbing CLC, $\gamma = 0$ in the general expression for the dielectric constant $\varepsilon = \varepsilon_0(1 + i\gamma)$. (We note that in real situations, $|\gamma| \ll 1$.) The calculations of the reflection R and transmission T coefficients as functions of the frequency in accordance with Eqs. (10) (Figs. 2a and 3a) give the well-known results [17–21]: a strong reflection inside the stop band, frequency oscillations of T and R outside the stop-band edges with $0 \le R \le 1$, and the preservation of the relation $T + R = 1$ for all frequencies. This means that $T = 1$ at the frequencies corresponding to $R = 0$ (see Fig. 3).

The corresponding calculations of the amplitudes E_+^+ and E_-^+ of the eigenwaves excited in the layer (Figs. 2*b,c* and 3*b,c*) reveal a nontrivial frequency dependence of E_+^+ and E_-^+. Namely, close to the stop-band edges (outside the stop-band edges), frequency oscillations of the amplitudes are accompanied by an essential enhancement of their magnitude relative to the incident wave amplitude (in the calculations, the incident wave amplitude is assumed to be equal to 1). The thicker the layer, the higher is the enhancement (cf. Figs. 2 and 3). As Figs. 2 and 3 show, the positions of the amplitude oscillation maxima just coincide with (or are very close to, for an absorbing or amplifying CLC) the positions of the reflection coefficient minima corresponding to $R = 0$ for a nonabsorbing CLC.

The above relation between the amplitudes of eigenwaves and incident waves at the specific frequencies shows that for these frequencies, the energy of radiation in the CLC at a given layer thickness is much higher than the corresponding energy of the incident wave at the same thickness. Hence, in complete accordance with Ref. [1], we conclude that at the corresponding frequencies, the incident wave excites some localized mode in the CLC. To find this localized mode, we have to solve homogeneous system (7), i. e., Eqs. (7) with zero values of E_{ir} and E_{il}. The solvability condition for the obtained homogeneous system determines the discrete frequencies of these localized modes:

$$\mathrm{tg}(qL) = \frac{i(q\tau/\kappa^2)}{(\tau/2\kappa)^2 + (q/\kappa)^2 - 1}. \qquad (13)$$

In the general case, solutions of Eq. (13) for the EM frequencies can be found only numerically. The EM frequencies ω_{EM} turn out to be complex quantities, which can be represented as $\omega_{EM} = \omega_{EM}^0(1 + i\Delta)$, where Δ is a small parameter in real situations. Therefore, the localized modes weakly decay in time, i. e., are quasistationary modes. Fortunately, an analytic solution can be found in a certain limit case, namely, for a sufficiently small Δ ensuring the condition $L\,\mathrm{Im}\,q \ll 1$. In this case, the ω_{EM}^0 values coincide with the frequencies of zero values of the reflection coefficient R for a nonabsorbing CLC, determined by the conditions

$$qL = n\pi, \quad \Delta = -\frac{\delta(n\pi)^2}{2(L\delta\tau/4)^3}, \qquad (14)$$

where n is the EM number, which increases as the frequency departs from the stop-band edge ($n = 1$ corresponds to the frequency closest to the stop-band edge).

In the found solution of homogeneous system (7), the ratio of the eigensolution amplitudes is $E_-^+/E_+^+ = -1$ and the field distribution inside the CLC layer is a superposition of two eigenwaves given by Eq. (2) with this amplitude ratio. The explicit expression for the EM field distribution inside the CLC layer following from Eq. (2) is

$$\mathbf{E}(\omega_{EM}, z, t) = i\exp(-i\omega_{EM}t) \times \\ \times \left\{ \mathbf{n}_+ \exp\left(\frac{i\tau z}{2}\right)\sin(qz) + \frac{\mathbf{n}_-}{\delta}\exp\left(-\frac{i\tau z}{2}\right) \times \right. \\ \left. \times \left\{ \left[\left(\frac{\tau}{2\kappa}\right)^2 + \left(\frac{q}{\kappa}\right)^2 - 1 \right] \sin(qz) - \frac{i\tau q}{\kappa^2}\cos(qz) \right\} \right\}, \qquad (15)$$

where q is determined by Eq. (11). For the analytic solution mentioned above, Eq. (15) for the EM field distribution inside the CLC layer becomes

$$\mathbf{E}(\omega_n, z, t) = i\exp(-i\omega_n t) \times \\ \times \left\{ \mathbf{n}_+ \exp\left(\frac{i\tau z}{2}\right)\sin\left(\frac{n\pi z}{L}\right) + \frac{\mathbf{n}_-}{\delta}\exp\left(-\frac{i\tau z}{2}\right) \times \right. \\ \times \left\{ \left[\left(\frac{\tau}{2\kappa}\right)^2 + \left(\frac{n\pi}{L\kappa}\right)^2 - 1 \right] \sin\left(\frac{n\pi z}{L}\right) - \right. \\ \left. \left. - \frac{i\tau n\pi}{L\kappa^2}\cos\left(\frac{n\pi z}{L}\right) \right\} \right\}, \qquad (16)$$

where ω_n corresponds to a zero value of R (i. e., ω_n is determined by $qL = n\pi$). The eigensolution of the boundary value problem given by Eqs. (15) and (16) is a standing wave localized at the layer thickness L with the amplitude modulated along z axis. The number of modulation periods at the layer thickness L coincides with the EM number n.

The EM total field (the sum of the fields of two eigenmodes in Eqs. (15) and (16)) at any coordinate z

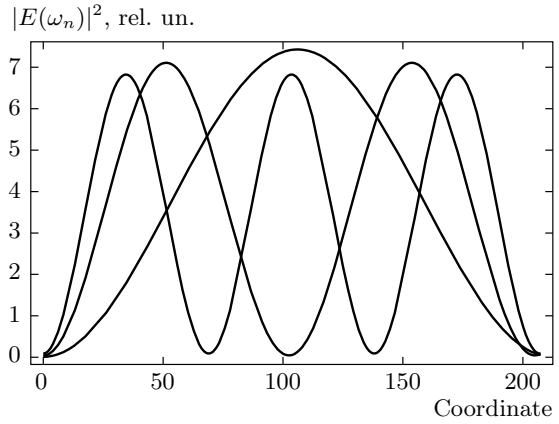

Fig. 4. The calculated EM energy distributions inside the CLC layer versus coordinate (in the dimensionless units $z\tau$) for the first three EMs ($\delta = 0.05$, $N = 16.5$, $n = 1, 2, 3$)

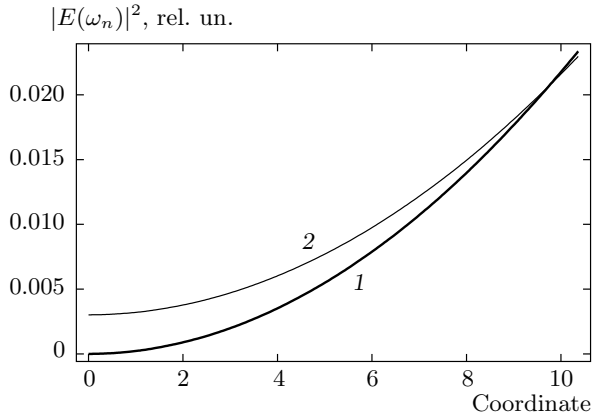

Fig. 5. The calculated EM energy distributions close to the CLC layer surface versus coordinate (in the dimensionless units $z\tau$) for a plane wave directed inside (*1*) and outside (*2*) the layer for the first EM ($\delta = 0.05$, $N = 16.5$, $n = 1$)

in the layer makes a fixed angle to the local director direction, i. e., the field in the layer rotates together with the director as a function of z and performs the same number of rotations as the director does at the layer thickness. The field distributions following from Eqs. (15) and (16) for the EM numbers $n = 1, 2, 3$ are presented in Fig. 4. The figure shows that the EM field is localized inside the CLC layer and its energy density experiences oscillations inside the layer with the number of oscillations equal to the EM number n. We note that the figure presents the total energy distribution in the layer. However, as is clear from Eqs. (2), (15), and (16), the total field at each point of the CLC layer is represented by two plane waves propagating in the opposite directions, and hence the intensities of the waves propagating in opposite directions can be calculated separately at any point in the layer. In general, the coordinate distribution of the intensities of waves propagating in opposite directions is similar to the distribution presented in Fig. 4. But these distributions are of a special interest close to the layer surfaces. Figure 5 shows the intensity coordinate distributions of the waves propagating inside and outside the layer close to the layer surfaces. We can see that at the layer surface, the intensity of the wave propagating inside the layer is strictly zero, but the intensity of the wave propagating outside the layer is nonzero (although small). This means that the EM energy is leaking from the layer through its surfaces. Equation (16) implies the expression

$$E_{out} = \frac{\tau n \pi}{\kappa^2 L \delta} \approx \frac{np}{L\delta} \tag{17}$$

for the leaking wave amplitude at the CLC layer surface, where p is the CLC pitch. Equation (17) shows that the EM energy leakage is inversely proportional to the squared layer thickness L and proportional to the squared EM number n. Hence, the most long-lived is the first EM in a CLC layer. If $L\delta/p \gg 1$, the leaking wave amplitude E_{out} is small ($E_{out} < 1$), as Eq. (17) shows.

For a nonabsorbing CLC layer (which is under consideration in this section), the only source of decay is the energy leakage through its surfaces; the decrease in the EM energy in unit time is equal to the energy flow $(2c/\sqrt{\varepsilon_0})|E_{out}|^2$ of the leaking waves, and therefore, using Eqs. (15)–(17), we easily obtain the EM lifetime τ_m as

$$\tau_m = \int |\mathbf{E}(\omega_{EM}, z, t)|^2 dz \times \left\{ \frac{d}{dt} \int |\mathbf{E}(\omega_{EM}, z, t)|^2 dz \right\}^{-1} \approx \approx \frac{5}{16} \frac{L\sqrt{\varepsilon_0}}{c} \left[1 + \frac{4}{5} \left(\frac{L\delta}{pn} \right)^2 \right]. \tag{18}$$

Under the condition $L\delta/pn \gg 1$, Eq. (18) reduces to

$$\tau_m \approx \frac{1}{4} \frac{L\sqrt{\varepsilon_0}}{c} \left(\frac{L\delta}{pn} \right)^2. \tag{19}$$

Hence, for sufficiently thick CLC layers, as their thickness L increases, the EM lifetime τ_m increases as the third power of the thickness and is inversely proportional to the square of the EM number n. We note that the same dependence of the lifetime τ_m on n and L follows from Eq. (14):

$$\tau_m \approx \frac{1}{\operatorname{Im} \omega_{EM}} = \frac{L}{c} \left(\frac{L\delta}{pn} \right)^2. \tag{20}$$

5. EXCITATION OF EDGE MODES

The analysis of the localized EM (solution of the homogeneous system following from Eqs. (7)) in the previous sections together with the solution of inhomogeneous equations (7) found in the previous sections allows discussing the ways and efficiency of the EM excitation. Excitation of the EM in a nonamplifying CLC layer requires an external wave (waves) of the frequency coinciding with the EM frequency incident at the CLC layer. The general solution of the boundary value problem found from system (7) in this case may be represented as a superposition of the particular solution corresponding to the inhomogeneous system (7) and the

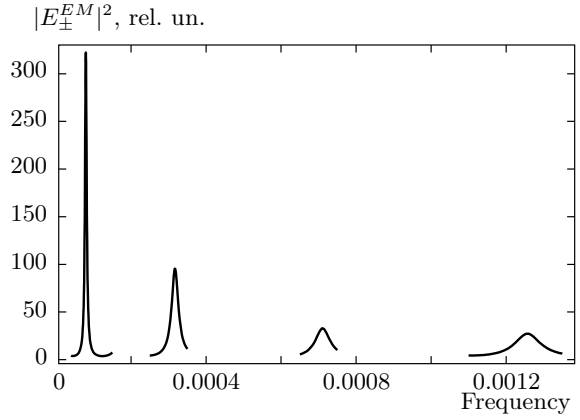

Fig. 6. The calculated squared amplitude of the EM close to the four EM frequencies ($\delta = 0.05$, $N = 350$)

solution corresponding to the homogeneous system (7), i. e., corresponding to the EM, with the coefficient to be determined from the boundary conditions. One can easily construct such a repesentation of the boundary value problem solution determined by Eqs. (12).

For this, it is sufficient to represent $E_{\pm}^{+}$ in the form $E_{\pm}^{+} = E_{\pm}^{EM} + E_{\pm}^{p}$, where $E_{\pm}^{EM}$ and $E_{\pm}^{p}$ are the respective amplitudes of eigenwaves in the EM and in the particular solution. Taking into account that the amplitudes $E_{\pm}^{EM}$ satisfy Eqs. (7) with zero right-hand sides, we obtain

$$E_{\pm}^{EM} = \pm E_{+}^{+}\left[1 + i\,\mathrm{tg}(qL)\right] \tag{21}$$

for the frequencies close to ω_{EM}. The $E_{\pm}^{EM}$ values calculated according (21) are presented in Fig. 6. Comparing Fig. 6 and Figs. 2 and 3 shows that for a sufficiently thick LC layer, the amplitudes $E_{\pm}^{+}$ are a very good approximation to $E_{\pm}^{EM}$.

The above results relate to a stationary process of EM excitation, i. e., to the situation of a plane wave of a fixed amplitude incident on a CLC layer. The formulas obtained can be used for finding the probability of EM excitation by a single photon. This probability is given by

$$W_{EM} = \frac{(1-R)\int \left|\mathbf{E}^{EM}(\omega,z,t)\right|^2 dz}{\int \left|\mathbf{E}^{EM}(\omega,z,t)\right|^2 dz + \int \left|\mathbf{E}^{p}(\omega,z,t)\right|^2 dz}, \tag{22}$$

where the integration is taken over the CLC layer thickness and $\mathbf{E}^{p}(\omega,z,t)$ is a particular solution of Eq. (6).

It turns out that if a plane wave (with unit amplitude) is incident on the CLC layer, the eigenmode amplitudes in the excited EM are given by the expressions for $E_{\pm}^{EM}$ above. But in this case, it is impossible to excite the EM only. It is accompanied by the particular solution of Eq. (6) with a nonzero amplitude determined by the relation $E_{\pm}^{+} = E_{\pm}^{EM} + E_{\pm}^{p}$. Hence, the efficiency of the EM excitation by one plane wave (the ratio of the squared EM amplitude to the squared incident wave amplitude) for the specific values of the relevant parameters may be estimated by the squared E_{+}^{+} value in Figs. 2*b* and 3*b*. The values of $E_{\pm}^{EM}$ close to the EM frequencies are more accurately determined by Eq. (21) (see also Fig. 6).

6. ABSORBING CLC

We now examine EMs in an absorbing CLC. The motivation for this study, in particular, is the DFB lasing in a CLC. It must be kept in mind that under lasing, a CLC is an essentially absorbing medium for the pumping wave. We examine the formulas in the previous sections in more detail with regard to their application to the pumping wave. We assume for simplicity that the absorption in the CLC is isotropic. We define the ratio of the imaginary part of the dielectric constant to its real part as γ, i. e., $\varepsilon = \varepsilon_0(1 + i\gamma)$. In actual situations, $\gamma \ll 1$. In Figs. 7–9, the R, T, and $1 - R - T$ frequency dependences are presented for several values of positive and negative γ including its values close to the threshold values for EMs (see Eq. (25) below). Due to the assumed isotropy of the absorption, the frequency dependences of the calculated characteristics are symmetric relative to the Bragg frequency (the middle point of the stop band), and therefore only the frequencies above the Bragg frequency are presented in the figures.

It is reasonable to comment here on the numerical values of the parameters used in calculations. The dielectric anisotropy is taken as $\delta = 0.05$, which corresponds to a typical value of this parameter. The same may be said about the layer thickness L. Because $\tau = 4\pi/p$, where p is the cholesteric pitch, the number of pitches N at the layer thickness L is equal to $l/4\pi$ ($l = L\tau$) and hence the value $l = 300$ accepted in calculations corresponds to N close to 30, i. e., to a number very common for experiments. All the mentioned quantities reveal frequency beats close to the frequency edge of the selective reflection band. The positions of the corresponding maxima and minima are determined by the layer thickness L, by δ, and are slightly dependent

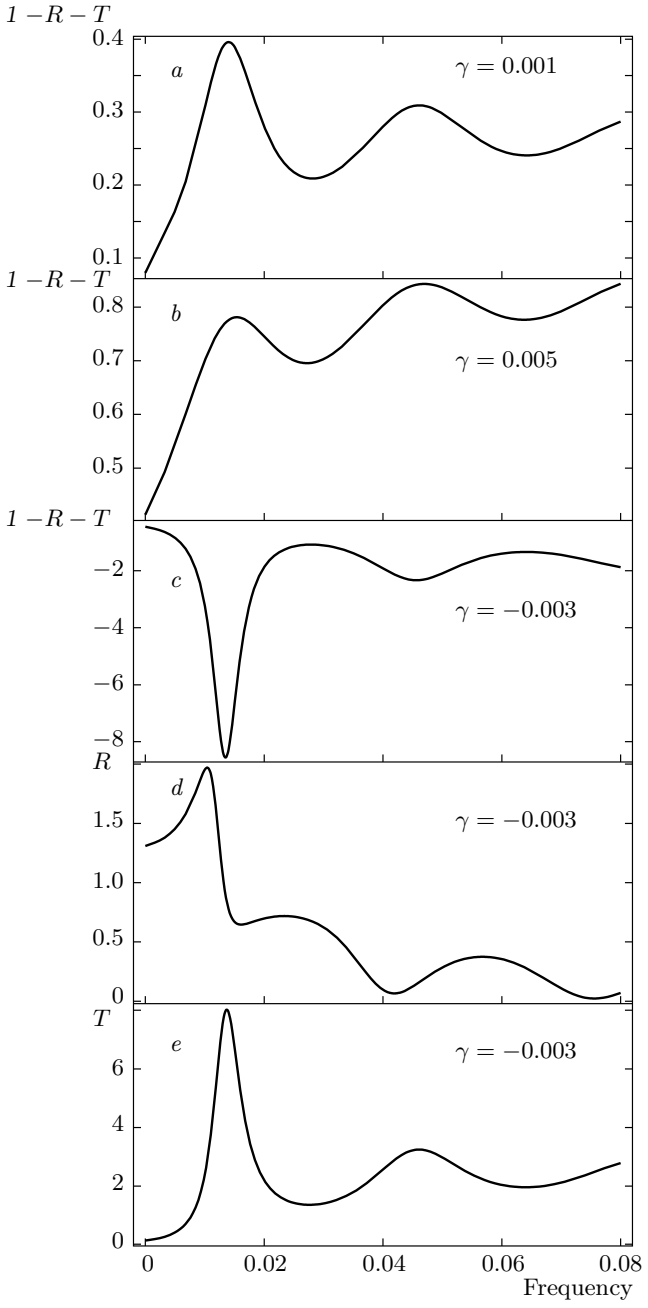

Fig. 7. Calculated frequency dependences ($l = L\tau = 4\pi N = 300$, $\delta = 0.05$) for absorption (a,b, and c), reflection (d), and transmission (e) in cases of low absorption (a and b) and low amplification below the threshold gain for the first lasing EM (c–e)

on the value of γ. In an absorbing CLC, the sum of the intensities of the reflected and transmitted beams is less than the intensity of the incident beam, i. e., $R+T<1$. The equality holds only for a nonabsorbing CLC. As an example, the positions of minima of the reflection coefficient R beats (following from Eq. (10)) are given above in Fig. 2a for a nonabsorbing CLC, i. e., for $\gamma = 0$, which correspond to

$$\begin{gathered} qL = \pi n, \quad \pm\nu = 1 + (\pi n/a)^2/2, \\ n = 1, 2, 3, \ldots, \quad \nu = 2(\omega - \omega_B)/\omega_B\delta, \\ \omega_B = c\tau/2\sqrt{\varepsilon_0}, \quad a = \tau L\delta/4. \end{gathered} \tag{23}$$

In a typical situation, $a \gg 1$.

The edges ω_e of the selective reflection band are related to the Bragg frequency ω_B as

$$\omega_e = \frac{\omega_B}{\sqrt{1 \pm \delta}} = \frac{c\tau}{2\sqrt{\varepsilon_0(1 \pm \delta)}}. \tag{24}$$

Hence, ν at the edges is given by $\nu_e = \delta/2\left(\sqrt{1 \pm \delta} - 1\right) \approx \mp 1$.

For small γ and $L\,\mathrm{Im}\,q \ll 1$, the reflection and transmission coefficients (10) at frequencies (23) of the reflection minima become

$$\begin{gathered} R = \frac{(a^3\gamma)^2}{\left[(n\pi)^2 + a^3\gamma\right]^2}, \\ T = \frac{(n\pi)^4}{\left[(n\pi)^2 + a^3\gamma\right]^2}, \\ R + T = 1 - \frac{2(n\pi)^2 a^3\gamma}{\left[(n\pi)^2 + a^3\gamma\right]^2}. \end{gathered} \tag{25}$$

It follows from Eqs. (23) and (25) that for each n, the maximum absorption, i. e., maximum $1-R-T$, occurs for $(n\pi)^2 = a^3\gamma$. This means that the maximum absorption occurs for a special relation between δ, γ, and L and if this relation, i. e., $(n\pi)^2 = a^3\gamma$, is fulfilled, then $R = 1/4$, $T = 1/4$, and $1 - R - T = 1/2$. Because of the assumed smallness of γ, this result corresponds to a strong enhancement of the absorption for weakly absorbing layers.

As was shown in Refs. [9, 10], just at the frequency values determined by Eq. (23), the effect of anomalously strong absorption reveals itself for an absorbing CLC (Figs. 7a,b) and the edge modes for an amplifying CLC reveal themselves at lasing [1] (Fig. 8) (see similar results for layered media in [14, 15]). Hence, to minimize the intensity of the pumping wave that ensures lasing in a CLC, it is desirable to perform the pumping in conditions of the anomalously strong absorption effect and realization of lasing in the EM. These options were investigated in detail in Refs. [11, 12] and are briefly discussed in the following sections. In the conclusion of this section, the following observation should be made (cf. Figs. 7–9): the absorption maxima in the frequency dependences are not so sharp as the intensity maxima for the lasing modes.

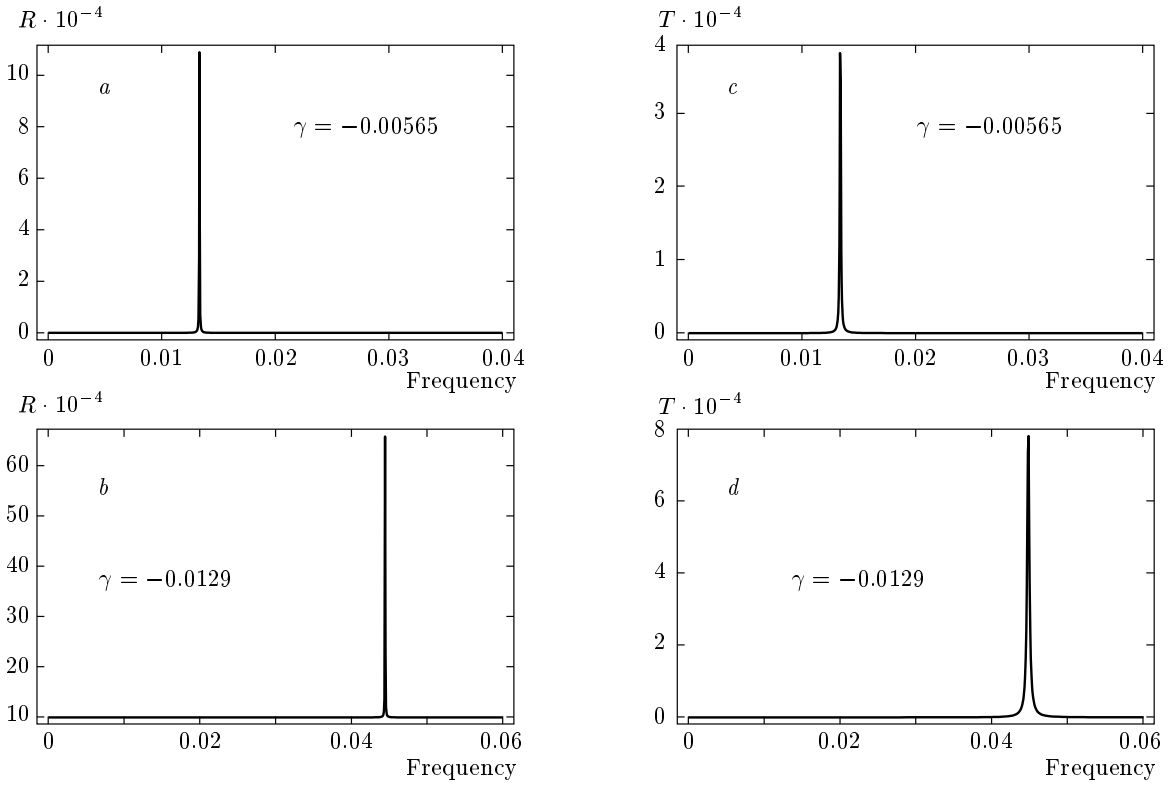

Fig. 8. Calculated frequency dependences ($l = 300$, $\delta = 0.05$) for coefficients of reflection (a and b) and transmission (c and d) close to the threshold gain for the first (a and c) and the second (b and d) lasing EMs

7. AMPLIFYING CLC

We now assume that $\gamma < 0$, which means that the CLC is amplifying. If $|\gamma|$ is sufficiently small, the waves emerging from the layer according to Eqs. (7)–(10) exist only in the presence of at least one external wave incident on the layer, and their amplitudes are determined by the solution of Eqs. (7) and (9). In this case (see Fig. 9*c*), $R + T > 1$ or $1 - R - T < 0$, which just corresponds to the definition of an amplifying medium.

However, if the imaginary part of the dielectric tensor, i. e., γ, reaches some critical negative value, the quantity $R + T$ diverges and the amplitudes of waves emerging from the layer are nonzero even for zero amplitudes of the incident waves. This happens when the determinant of Eq. (7) vanishes. At this point, of course, the amplitudes of emerging waves are not determined by solution (9) of linear equations (1) (a nonlinear problem should then be solved). But as we saw above, the vanishing points of the determinant of Eq. (7) determine the EMs [1, 14, 15] and the corresponding values of the gain (or the negative imaginary part of the dielectric tensor), i. e., the minimum threshold gain at which the lasing occurs (see the corresponding discussion for scalar periodic media in Refs. [14, 15]).

Therefore, the equation determining the threshold gain (γ) at which the lasing occurs (zero value of the determinant of Eq. (7) or of the denominator in Eq. (10)) turns out to coincide with Eq. (13). It must be solved now not for the frequency but for the imaginary part of the dielectric constant (γ). In the general case, this equation has to be solved numerically. However, for a very small negative imaginary part of the dielectric tensor, the EM frequencies are pinned to the frequencies of zeros of the reflection coefficient in its frequency beats outside the stop-band edge for the same layer with a zero imaginary part of the dielectric tensor [1, 9, 10]. This is why the threshold values of the gain for the EMs can be represented by analytic expressions in this limit case.

For small $|\gamma|$ and $L|\operatorname{Im} q| \ll 1$, the reflection and transmission coefficients in Eq. (10) at the frequencies (23) of reflection minima are reduced again to expressions (25), although with negative γ.

Hence, R and T may be divergent, and the points of their divergence correspond to the lasing at the EM frequencies and determine the corresponding values of

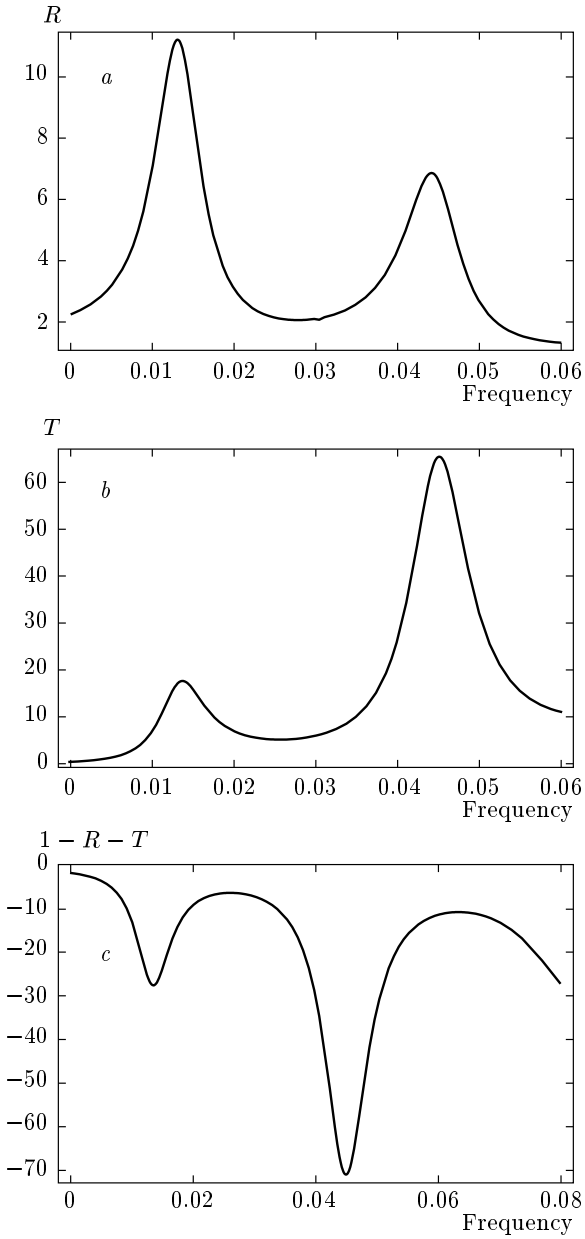

Fig. 9. R (a), T (b), and $1-R-T$ (c) calculated versus the frequency ($l = 300$, $\delta = 0.05$) for $\gamma = -0.009$, i. e., for the gain between the thresholds for the first and the second lasing EMs

the threshold γ, i. e., a minimum $|\gamma|$ at which the lasing occurs for nth reflection minimum:

$$\gamma = -\frac{(n\pi)^2}{a^3} = -\frac{\delta(n\pi)^2}{(\tau L\delta/4)^3}\,. \qquad (26)$$

As can be seen from Eq. (26), the threshold values of $|\gamma|$ are inversely proportional to the third power of the layer thickness and the minimum value of $|\gamma|$ corresponds to $n = 1$, i. e., to the edge lasing mode closest to the selective reflection band edge (cf. analogous results for scalar layered media in [14, 15]). The values of γ given by Eq. (26) is convenient to use for estimating the threshold values of γ in the general case and as a zero approximation in the numerical solution of Eq. (13) for the threshold values. The frequency distances between the consequent EMs are equal to

$$\nu_{n+1} - \nu_n = \frac{1}{2}\left(\frac{\pi}{a}\right)^2 (2n+1),$$

i. e., are inversely proportional to the second power of the layer thickness (cf. the corresponding distance between the lasing frequencies in a homogeneous layer, which is inversely proportional to the layer thickness).

It also follows from Fig. 8 that the different threshold values of γ correspond to the different EMs (divergent R and T) in Fig. 8. This means that separate lasing modes can be excited by changing the gain (γ). If the value of γ is between the consecutive threshold values of γ for neighboring lasing modes, the lasing may not be achieved and the layer may reveal only amplifying properties (see Fig. 9). This means that changing the pumping wave intensity allows achieving lasing at the individual EM and that the lasing intensity is not a monotonic function of the pumping intensity. Because the lasing frequency is determined by the EM frequencies, there is an option for some variation of the lasing frequency inside the width of the dye line by changing the CLC pitch by means of temperature variations [6, 7] or by application of an external electric or magnetic field to the layer [4]. We note that smooth variations of the external agent may result in jump-like variations of the lasing frequency [22] related to the jumps of the CLC pitch, which are sensitive to the surface anchoring [23].

8. OPTIMIZATION OF PUMPING

The formulas in the previous sections allow optimizing the lasing threshold separately by reaching a coincidence of the lasing frequency with the frequency of the first EM and optimizing the pumping efficiency by reaching a coincidence of the pumping frequency with the frequency of the first maximum in the anomalously strong absorption effect [9]. We note that the same CLCs must simultaneously be an absorbing material at the pumping frequency and amplifying one at the lasing frequency. In the present section, we discuss the possibilities to simultaneously reach the highest efficiency of the pumping and the lowest value of the lasing threshold gain. The requirements of the highest efficiency of

the pumping and the lowest value of the lasing threshold gain are contradictory for a collinear geometry because they assume that the lasing frequency ω_l and the pumping frequency ω_p practically coincide with the frequency edges of the selective reflection band. However, the lasing frequency ω_l is less than the pumping frequency ω_p. We note that this contradiction for the collinear geometry may be overcame by a lucky chance or by a very fine tuning of the lasing parameters if the difference $\omega_p - \omega_l$ is small and ω_p coincides with the high-frequency edge of the reflection band and ω_l coincides with the low-frequency edge of the reflection band, which results in the following frequencies of the lasing and pumping waves:

$$\omega_p = \frac{c\tau/2}{\sqrt{\varepsilon_{0p}(1-\delta_p)}}, \quad \omega_l = \frac{c\tau/2}{\sqrt{\varepsilon_{0l}(1+\delta_l)}}, \qquad \frac{\omega_p}{\omega_l} = \sqrt{\frac{\varepsilon_{0l}(1+\delta_l)}{\varepsilon_{0p}(1-\delta_p)}}, \tag{27}$$

where the dielectric constant ε_0 and the anisotropy δ are marked by subscripts «p» and «l» relating to the frequency dispersion of the dielectric properties and meaning that the respective parameters are to be taken at the pumping and lasing frequencies. We note that a decrease in the lasing threshold due to the anomalously strong absorption of the pumping wave in the collinear geometry was recently observed experimentally in Ref. [13].

Another possibility to reach the lowest threshold in the collinear geometry may be realized by applying an external electric (or magnetic) field to the LC material. It is known [10] that in this case, due to the distortion of the LC helix, many diffraction orders exist for light propagating along the helix axis and the pumping and lasing frequencies may be fitted to the frequencies of different diffraction orders. Nevertheless, the fitting again requires a very fine tuning of the lasing parameters.

However, there is a regular way to optimize the pumping intensity (under the assumption that the lasing occurs along the helical axis). There is an option to use a noncollinear pumping without any tuning of the lasing parameters, i. e., with the pumping wave propagating at an angle to the helical axis, which allows the pumping wave to satisfy the conditions of the anomalously strong absorption effect. A rough estimate derived from the fact that the lasing and pumping waves experience Bragg scattering gives the following value of the angle θ between the pumping wave propagation direction and the helical axis:

$$\theta = \arccos(\omega_l/\omega_p). \tag{28}$$

To obtain a more accurate expression for the pumping wave propagation direction, one has to solve the Maxwell equations for light propagating at an angle to the helical axis and find the angle θ corresponding to the conditions of the anomalously strong absorption effect [9, 10]. Unfortunately, no exact analytic solution of the Maxwell equations is known in this case and therefore a numerical approach has to be used. The full power of the numerical approach manifests itself if the frequency dispersion of the dielectric constant and of the LC dielectric anisotropy are taken into account. However, these quantities are usually not very well known, and hence in the experiment, even if the calculated angle θ is known, the actual angle of the anomalously strong absorption effect is sought by changing the pumping wave propagation direction due to the mentioned uncertainties.

Under these circumstances, an approximate expression for θ more accurate than (28) may be quite useful. The corresponding expression was found [11, 12] in the framework of the dynamical theory of diffraction applied to the case of light propagating at an angle to the helical axis [10, 21, 24]. The dielectric anisotropy δ plays the role of a small parameter in this theory. Because the dielectric anisotropy δ is quite small in many practical cases ($\delta < 0.1$), the accuracy of the results found in the framework of the dynamical theory may be sufficient to describe the experimental results.

9. CALCULATION RESULTS

To obtain the gain γ that corresponds to the onset of lasing in an CLC layer, we investigated the behavior of the R (reflection) and T (transmission) coefficients. The divergence of R and T corresponds to the lasing threshold value of γ. These divergences occur at the vanishing point of the determinant of Eq. (7). This condition gives a direct way to find the EM frequency corresponding to the solution of Eq. (13). In Fig. 10, the analytically found and numerically calculated threshold gains for the first three EMs are presented for several values of the parameter $L\delta/p$. The comparison demonstrates that the larger the parameter $L\delta/p$ is, the closer the analytically found and numerically calculated threshold gains are. For an amplifying

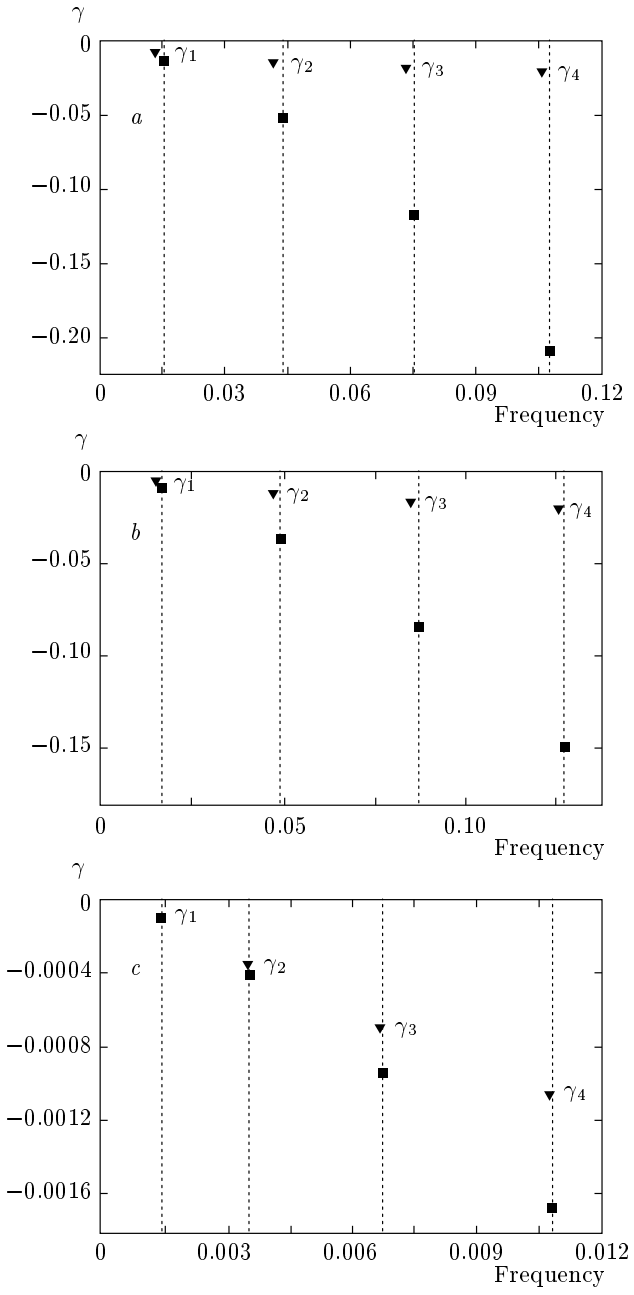

Fig. 10. Numerical (▼) and analytic (■) solutions of EM dispersion equation (13) for the parameter $L\delta/p = 0.9$, $\delta = 0.03$ (a), $L\delta/p = 1.193$, $\delta = 0.05$ (b), and $L\delta/p = 4.5$, $\delta = 0.03$ (c); a — $\gamma_1 = -0.00676$, $\gamma_2 = -0.01369$, $\gamma_3 = -0.01761$, and $\gamma_4 = -0.02009$; b — $\gamma_1 = -0.0057$, $\gamma_2 = -0.01305$, $\gamma_3 = -0.01775$, and $\gamma_4 = -0.02075$; c — $\gamma_1 = -0.000096$, $\gamma_2 = -0.000352$, $\gamma_3 = -0.000696$, and $\gamma_4 = -0.001066$

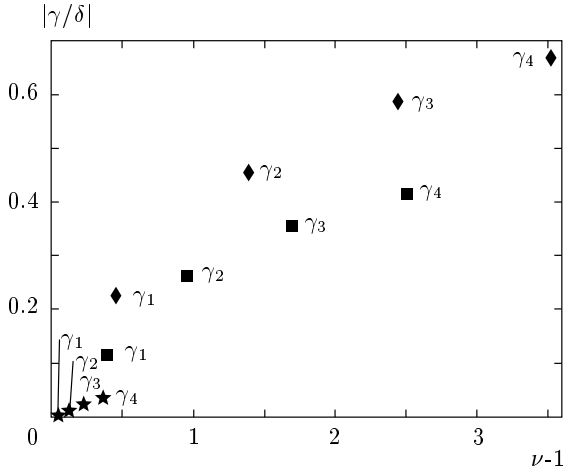

Fig. 11. Numerical solutions of EM dispersion equation (13) for the gain normalized by δ for $L\delta/p = 0.9$ (⧫), 1.193 (■), 4.5 (⋆). The found values of γ are also given for $\delta = 0.05$ (■ — $\gamma_1 = 0.0057$, $\gamma_2 = -0.01305$, $\gamma_3 = -0.01775$, and $\gamma_4 = -0.02075$) and $\delta = 0.03$ (⋆ — $\gamma_1 = -0.000096$, $\gamma_2 = -0.000352$, $\gamma_3 = -0.000696$, and $\gamma_4 = -0.001066$; ⧫ — $\gamma_1 = -0.00676$, $\gamma_2 = -0.01369$, $\gamma_3 = -0.01761$, and $\gamma_4 = -0.02009$)

CLC, the numerical solutions for the gain values normalized by δ (solutions of Eq. (13)) are presented in Fig. 11 for several values of the parameter $L\delta/p$ (the specific values of γ are also presented in Fig. 11 for $\delta = 0.05$ and $\delta = 0.03$). Zero values of the determinant of Eq. (7) occur at discrete values of γ and $\mathrm{Re}\,\omega$. Their values are found for several first EMs; calculations of R and T were also performed to control the solution procedure using the initial value of γ given by analytic expression (26). The final values of ω_i and γ_i were found by a graphical solution of the problem. The gain values normalized by δ for the fixed value of the parameter $L\delta/p$, presented in Fig. 11, allow recalculating γ for various values of δ and L corresponding to the same value of $L\delta/p$.

The ω_i values are very close to their values corresponding to zeros of the reflection coefficient R for a nonabsorbing CLC, determined by Eq. (14). The values of γ_i are close to the ones given by analytic expression (26) only for a sufficiently large parameter $L\delta/p$. On the whole, there is a general trend in the difference of the analytic and numerical solutions. The values of $\mathrm{Re}\,\omega_i$ found numerically are smaller than the analytic ones and the numerically found $|\gamma_i|$ are larger than the analytic ones (see Eq. (26)).

10. CONCLUSION

The performed analytic and numerical theoretical examination of the EMs in an LC allows representing the physics of these localized modes more clearly. We also note that the results obtained here for spiral media are relevant to any periodic media, and hence the qualitative description of the EMs in these media is the same as for the CLC and the analytic formula presented above may be used as a useful guide in studying other periodic media.

As regards the CLC, in particular, it turns out that there are some real possibilities related to these localized modes for reaching a higher efficiency of the DFB lasing in the CLC. Namely, possibilities of further reduction of the lasing threshold relative to the one already achieved were predicted [11, 12] and partially experimentally observed [13] as well as possibilities of varying the lasing frequency in this kind of lasing. It should be mentioned that an advantage of the CLCs compared to solid media consists in the fact that their parameters are easily variable. Hence, the CLC may be considered a convenient model object for studying the lasing in any periodic media, even in three-dimensional periodic structures (see Ref. [25] on lasing in the LC blue phase). Another fortunate circumstance from the theoretical standpoint is the availability of an exact analytic solution of the Maxwell equations for light propagating along the helical axis. For other periodic media, no exact analytic solution is known and the coupled wave approximation is usually applied to the problem [14, 15].

We note that the equations in the previous sections formally assuming a frequency-independent dielectric susceptibility and its isotropy may be easily generalized to the experimentally realizable case of the frequency-dependent dielectric susceptibility and its anisotropy. For this, the corresponding parameters in the equations are to be considered some functions of frequency. However, the question of the explicit expressions for these functions arises. It seems that the most pragmatic way to determine the corresponding frequency dependences is to obtain them from experimental measurements.

An essential point for the experimental observation of the examined anomalously strong absorption effect of the pumping wave is that the periodic structure be perfect enough for observing beats of the reflection coefficient at the edges of the reflection band. Insufficient perfection of the periodic structure leads to a decrease in the anomalously strong absorption. A similar decrease in the anomalously strong absorption is related to a finite frequency width of the pumping wave. The corresponding reduction of the absorption is the result of averaging the expressions presented above over the frequency width of the pumping wave line [9, 10]. A similar influence of the sample perfection on the decrease in the threshold lasing gain also takes place. We also note that the assumption accepted above regarding the absence of dielectric reflection on the boundaries of the CLC layer (the equality of the external dielectric and average dielectric constant of the CLC) requires a special experimental care. If this assumption is not met in an experiment, the reflection at the boundaries converts the diffracting polarization into the nondiffracting one, which also decreases the anomalously strong absorption and changes the polarization properties of the phenomenon.

Another accepted simplification of the problem is related to the assumption that the absorption in the CLC is isotropic. In some cases, this assumption may correspond to the real situation. But in the general case, the local absorption anisotropy in a CLC may be noticeable. Hence, the study of the problem in the case of anisotropic absorption is quite urgent.

And finally, as was already mentioned, because of the insufficiently precise knowledge of the CLC parameters, a practical way to observe the theoretically predicted effects in the experiment is a search for the effect by small variations of experimental parameters (propagation direction, temperature, etc.) around the values calculated according to formulas in the previous sections.

It should also be kept in mind that the EMs studied here reveal themselves not only in lasing but also in other optical phenomena. For example, the nonlinear optical harmonic generation [26] and Cherenkov radiation [27] in a periodic medium is enhanced at the EM frequencies (see also Figs. 29 and 32 in [10] and Figs. 5.10 and 6.2 in [21] related to the nonlinear optical harmonic generation and Cherenkov radiation in CLCs).

This work was supported by the RFBR (grant № 09-02-90417-Ukr_f_a).

REFERENCES

1. V. I. Kopp, Z.-Q. Zhang, and A. Z. Genack, Progr. Quant. Electron. **27**, 369 (2003).

2. I. P. Il'chishin, E. A. Tikhonov, V. G. Tishchenko, and M. T. Shpak, Pis'ma v Zh. Eksp. Teor. Fiz. **32**, 27 (1980).

3. B. Taheri, A. F. Muñoz, P. Palffy-Muhoray, and R. Twieg, Mol. Cryst. Liq. Cryst. **358**, 73 (2001).

4. M. Ozaki, M. Kasano, T. Kitasho et al., Adv. Mater. **15**, 974 (2003).

5. M. I. Barnik, L. M. Blinov, V. V. Lazarev et al., J. Appl. Phys. **103**, 123113 (2008).

6. S. M. Morris, A. D. Ford, M. N. Pivnenko, and H. J. Coles, J. Appl. Phys. **97**, 023103 (2005).

7. A. Chanishvili, G. Chilaya, G. Petriashvili et al., Appl. Phys. Lett. **86**, 055107 (2005).

8. H. Finkelmann, S. T. Kim, A. Muñoz et al., Adv. Mater. **13**, 1069 (2001).

9. V. A. Belyakov, A. A. Gevorgian, O. S. Eritsian, and N. V. Shipov, Zh. Tekhn. Fiz. **57**, 1418 (1987).

10. V. A. Belyakov and V. E. Dmitrienko, in Sov. Sci. Rev., Sec. A — Physics, Vol. 13, ed. by I. M. Khalatnikov, Harwood Acad. Publ. (1989), p. 80.

11. V. A. Belyakov, Mol. Cryst. Liq. Cryst. **453**, 43 (2006).

12. V. A. Belyakov, Ferroelectrics **364**, 33 (2008).

13. Y. Matsuhisa, Y. Huang, Y. Zhou et al., Appl. Phys. Lett. **90**, 091114 (2007).

14. H. Kogelnik and C. V. Shank, J. Appl. Phys. **43**, 2327 (1972).

15. A. Yariv and M. Nakamura, J. Quant. Electr. **QE-13**, 233 (1977).

16. J. P. Dowling, M. Scalora, M. J. Bloemer, and C. M. Bowden, J. Appl. Phys. **75**, 1896 (1994).

17. H. de Vries, Acta Cryst. **4**, 219 (1951).

18. E. I. Kats, Zh. Eksp. Teor. Fiz. **59**, 1854 (1971).

19. V. A. Belyakov and A. S. Sonin, *Optics of Cholesteric Liquid Crystals* (in Russian), Nauka, Moscow (1982).

20. P. G. de Gennes and J. Prost, *The Physics of Liquid Crystals*, Clarendon Press, Oxford (1993).

21. V. A. Belyakov, *Diffraction Optics of Complex Structured Periodic Media*, Springer-Verlag, New York, Ch. 4 (1992).

22. K. Funamoto, M. Ozaki, and K. Yoshino, Jpn. J. Appl. Phys. **42**, L1523 (2003).

23. V. A. Belyakov, I. W. Stewart, and M. A. Osipov, Phys. Rev. E **71**, 051708 (2005).

24. V. A. Belyakov and V. E. Dmitrienko, Fizika Tverdogo Tela **15**, 2724, 3540 (1973).

25. W. Cao, A. Muñoz, P. Palffy-Muhoray, and B. Taheri, Nature Mater. **1**, 111 (2002).

26. V. A. Belyakov and N. V. Shipov, Zh. Eksp. Teor. Fiz. **82**, 1159 (1982).

27. N. V. Shipov and V. A. Belyakov, Zh. Eksp. Teor. Fiz. **75**, 1589 (1978).